



## Silver Nitrate Particles nanotoxicity using Cell Culture and Apoptosis (Genetic and Cell Study)

### KEYWORDS

Silver nanoparticles, blood lymphocytes, genotoxicity, chromosomal aberrations, metaphase chromosomes, hemolysis

**Ragia M. Hegazy**

Department of Forensic Medicine & Clinical Toxicology, Benha Faculty of Medicine, ARE

**Eman Farouk**

Department of Histology and Genetics, Benha Faculty of Medicine, ARE

**Taghreed G. Kharboush**

Department of Microbiology and Virology Benha Faculty of Medicine, ARE

### ABSTRACT

The present study focuses on the nanoparticle interaction with human peripheral blood cells from genetic and ultra structure study. AgNPs genotoxicity and cytotoxicity had been tested in human peripheral blood lymphocytes culture through DNA fragmentation, chromosomal aberrations and electron microscope. Also, metal ion analysis was done to check the uptake of nanoparticles in the cell pellet of human peripheral blood cells. AgNPs proved to be genotoxic in human peripheral blood lymphocytes culture through the fragmentation of DNA, chromosomal aberrations and metal ion analysis. Aberrant cell damage was recorded to be 0, 8 and 24% for 5, 15 and 25 µg/mL of AgNPs respectively. Significant increase and decrease in CAs and MI, respectively. Marked alterations in the ultrastructure blood cells in the form of: apoptosis of leukocytes and destruction of erythrocytes membrane. Structural changes in chromosomes and chromatids were also recorded. AgNPs was found to be cytotoxic and genotoxic.

### 1. INTRODUCTION

Nano-geno-toxicology which has an extensive scope in the field of nanotechnology where the toxicological effects of the nanomaterials manufactured are studied. There are many studies so far conducted for the assessment of toxicity of various nanomaterials<sup>(1, 2)</sup>. There is also a rapid development in the field of nanotechnology which resulted in a vast array of nanomaterials with varying size, shape, surface charge, chemistry, coating and solubility behaviour for various applications. Nanoparticles which are less than 100 nm in one dimension at atomic, molecular and macromolecular scales differs in physical and chemical properties from its bulk form due to high surface to volume ratio and found to be a potent toxicant<sup>(3-8)</sup>. Silver was the second most referenced (used in 25 products) in various medical and general products due to its antibacterial properties followed by silica<sup>(9)</sup>, titanium dioxide<sup>(6)</sup>, zinc oxide<sup>(9)</sup> and cerium oxide<sup>(9)</sup>. AgNPs have been extensively studied for antimicrobial properties and used increasingly in many consumer products such as wound healing creams, deodorants, clothing materials, bandages, cleaning solutions, sprays, antimicrobial agents, catalysts, cosmetics, therapeutic agents, biosensors, biomaterials and house-hold products<sup>(10,11)</sup>. Over usage of AgNPs, had created negative impact on human and non-human<sup>(12)</sup>, in addition to the general toxic properties of nanomaterials, the knowledge of the possible interactions with DNA becomes essential, given the importance of the effects of genetic damage in human health<sup>(13-15)</sup>.

Thus, genotoxic effects are intimately related to the incidence of various genetic disorders like cancer and other health effects, such as infertility, aging, atherosclerosis and the occurrence of genetic disorders in subsequent generations, when germ cells have been affected. For all these reasons, extensive studies on the genotoxicity of nanomaterials are necessary. AgNPs are found highly toxic to bacteria, fungi, algae, fish, certain plants, mammalian cells where the toxicity of a metal nanoparticle is influenced by several factors like solubility, binding specificity to a biological site, and their ionic release .... etc. Many reports have been published on the fact that AgNPs are toxic to human cells<sup>(16,17)</sup>.

Eom and Choi, 2010 have reported on structural and numerical chromosomal alterations induced by metal and metal

oxide nanoparticles performed on in vitro chromosomal and bacterial assays<sup>(18)</sup>.

Sathya, et. al, 2010; have identified potential harmful effects of AgNPs on human health and a comprehensive toxicity assay conducted on human Jurkat T cells, by relating oxidative stress endpoints<sup>(19)</sup>.

In this work we aimed to study the effect of AgNPs on human peripheral blood through genetic and ultra structure study.

### 2. MATERIALS AND METHODS

#### 2.1. NANOPARTICLES AND REAGENTS

99.5% trace metals basis AgNPs (CAS Number: 7440-22-4) diameter of approximately <100nm was obtained from Sigma Aldrich, USA. The physical characterization of AgNPs: surface area 5.0 m<sup>2</sup>/g; density 10.49 g/cm<sup>3</sup>.

RPMI-1640 medium, Fetal bovine serum (FBS), Penicillin and Streptomycin were purchased from GIBCO. Phyto-haemagglutinin, colchicine, Hypotonic solution (KCl), Fixative (Methanol: Acetic acid: 3:1) were of analytical grade. All other chemicals used were of the highest purity available from commercial sources.

#### 2.2 NANOPARTICLE CHARACTERIZATION

The engineered AgNPs were suspended and dispersed in deionised water (Milli-Q) by means of using ultrasonic vibrations at 40% amplitude (Sonics®, Vibra-cell 130W, 20 kHz, USA) for 5-10 minutes to get three different concentrations of 5, 15, 25 µg/ml. AgNP dispersions were then characterized (200 – 700 nm) using UV-Vis spectrophotometer for its plasmon resonance peak (UV-Visible Double beam spectrophotometer, Systronics 2201, India). Dynamic Light Scattering measurements were done for the particle size distribution (90 Plus Particle Size Analyzer, Brookhaven Instruments Corporation, Holtsville, NY, USA). FT-IR analysis (Thermonicolor, Avatar-330) has been done to examine surface characteristics, various chemical and conformational properties of AgNPs. To confirm and clarify the size and morphology of Ag NPs, transmission electron microscopy (TEM) characterization was performed on a HITACHI H-600 transmission electron microscope operating at an accelerating voltage of 100 kV. Particles were spotted onto 300 mesh holey carbon-coated copper grids and dried prior to TEM imaging. Imaging was conducted in high-resolution mode at 100 kV.

## 2.3 TOXICITY STUDIES

### 2.3.1 Sample collection

Venous blood was drawn from ten healthy volunteers with informed consent (aged 21-25, non-smoking, non-alcohol consuming) in heparinised vacutainers. It was stored at 4°C until brought to laboratory. They divided into two equal groups, one as control group and other as tested AgNPs toxicity in blood culture group.

### 2.3.2 Culture medium

RPMI-1640 supplemented with Fetal Bovine Serum (25% v/v), 1mM glutamine and 2mM NaHCO<sub>3</sub> was used for the culture of blood cells. Phyto-hemagglutinin (PHA), served as the mitogen for stimulating the lymphocytes to enter into mitosis.

### 2.3.3 Lymphocyte culture

Chromosome spreads were made from Phyto-hemagglutinin (PHA) stimulated human peripheral blood lymphocytes.

**2.3.4 Culture Set up:** Peripheral blood mononuclear cells (PB-MCs), obtained from 10 mL blood from healthy donors, and were separated by Ficoll/Paque (BioWhittaker) density gradient centrifugation. Then, 1 × 10<sup>5</sup> cells were placed in a 24-well round-bottom plate containing 0.5 mL RPMI-1640 (Gibco BRL, Eggenstein, Germany) supplemented with 25% (v/v) of FBS, 1% (v/v) antibiotics (final concentrations of 100 IU/mL Penicillin G and 100 IU/mL streptomycin). Control wells include phytohemagglutinin (PHA) stimulated cells (Murex; Life Technology, Karlsruhe, Germany), unstimulated cells. Three replicate cultures were made for each individual concentration and exposure time, and incubated at 37°C in a chamber containing 5% CO<sub>2</sub>. The results are expressed as the mean value of at least triplicate cultures. After a 24-h and 48-h culture period, the lymphocyte cultures were exposed to respective concentration of AgNPs. 5, 15, 25 µg/mL of AgNPs were added to respective culture tubes. This will give a 48 hr and 24 hr exposure of the nanoparticle to the lymphocyte culture respectively. At 67<sup>th</sup> hr of incubation period, the dividing cells were arrested at a stable metaphase stage by adding 0.025 µg/mL colchicine solution to each well. The cultures were incubated further for 5 hours at 37°C. Lymphocyte cultures were then harvested at 72 h. The cells were collected by centrifugation at 1000 rpm for 10 mins and washed twice with RPMI-1640 with L-glutamine, supplemented with 2% (v/v) FCS. The supernatant was aspirated, after gently tapping the cells containing pellet. 5ml of pre-warmed (37°C) hypotonic solution (0.075M KC1) was added to the tubes and the contents were mixed gently using a Pasteur pipette and incubate for 5 minutes at 37°C (20, 21). The cells were smeared and fixed onto slides with freshly prepared Carnoy's fixative (3:1: Methanol: Glacial acetic acid) at 20°C for one hour. A test slide was prepared by placing 100 µl of the cell suspension on a clean glass slide and dried immediately by using hot plate at 40°C. Staining was achieved with 10% (v/v) Giemsa in phosphate buffer pH 6.8 for 8 to 5 min. The test slides were examined under the microscope for cell density and metaphase spreads.

### 2.3.5 Preparation of Giemsa stain:

4% working solution was prepared by mixing 2ml of Giemsa stock solution and 2ml of 10% disodium hydrogen phosphate which was made up to 50ml with double distilled water. The test slides were stained in Giemsa solution for 5 minutes and washed in distilled water for 2 minutes and air dried.

**2.3.6 Scoring and microphotography** A 100 well spread metaphase from each animal were analyzed for CAs. Mitotic index (MI) for each group was also analyzed. The mitotic activity was estimated as the percentage of dividing cells to the total number of the examined cells (1000 cells per animals). A minimum of 50 good metaphase spreads were analysed in each sample for each concentration for CAs. Mitotic index (MI) was also analyzed. The mitotic activity was estimated as the percentage of dividing cells to the total number of the examined cells (20).

Scoring of chromosomal aberrations including stickiness and chromosomal breaks and gaps were carried out in well spread and stained cells was observed under oil immersion lens (100X) of the light microscope (Olympus, CX 31, USA). The selected metaphase spreads were photographed using

Cytovision software.

## 2.4 METAL ION ANALYSIS

Centrifugation was done at 12,000 rpm for 10 minutes, the clear supernatant was filtered through 0.22 µm (Anapore) membrane disc. To it, 2 ml of 1% nitric acid was added and the released ions were measured using AAS (Varian, AA-240) (22, 23).

## 2.5 HEMOLYSIS ASSAY

Erythrocyte suspension were washed by iso-osmotic PBS (PH 7.4) and then diluted in washing solution at the concentration of 500 µl and stored in 4°C for not more than 24 hours. 500 µl of erythrocyte suspension was interacted with AgNPs at the final doses (5, 15 & 25 µg/ml) and incubated for 1 h at 4°C. The erythrocyte treated with PBS (PH 7.4) was taken as the control. The degree of haemolysis was determined by a spectrophotometer through measuring the absorbance of the supernatant at 540 nm, after centrifuged. The absorbance of the control group was used as the blank as previously reported (24).

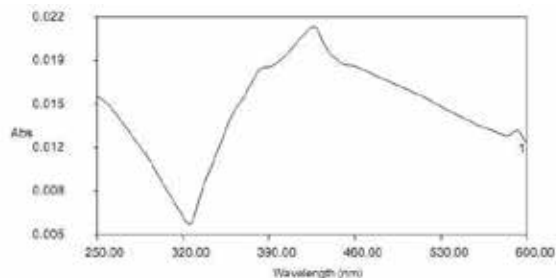
## 2.6 ELECTRON MICROSCOPY

Heparinized two millilitres of blood were immediately centrifuged, plasma was discarded and two cell layers were identified. The layer of white blood cells and thrombocytes plus an small portion of the red blood cells layer were removed and fixed primarily in phosphated buffered glutaraldehyde 2% (0.1M-pH 7.4), during 12 hours at 4°C. Samples were gently centrifuged and washed three times for 15 minutes in the same solution. Buffered 2% osmium tetroxide was used as secondary fixative during 4 hours, and subsequently cells were washed three times in distilled water for 15 minutes and left 4 hours in 1% uranyl acetate solution. Samples were dehydrated in ethanol (20<sup>i</sup>, 40<sup>i</sup>, 60<sup>i</sup>, 70<sup>i</sup>, 100<sup>i</sup> series) and passed through ethanol-propylene oxide, propylene oxide and propylene oxide-Embed812 resin. Samples were polymerized in fresh Embed resin, and were cut on an ultramicrotome (Reichert, Bensheim, Germany). Finally, the sections were stained with uranyl acetate (1% methanol) and Statos lead solution. Sections were examined with transmission electron microscope and images were taken with an EM digital camera system (MegaView, analysis© docu 3.2, Olympus Soft Imaging Systems GmbH, Münster, Germany) according to Bozzola, and Russell, 1999 (25).

**2.7 ETHICAL APPROVAL:** An ethical approval for this study from Ethics Committee in UQU, Faculty of Medicine and all subjects provided written informed consent about the aim of the study had obtained before conduction of the study.

**2.8 STATISTICAL ANALYSIS :** Statistical analysis was performed with SPSS (Version 12). Statistical evaluation was performed by analysis of two-tailed Student's t-test or analysis of variance (ANOVA) following multiple comparison tests. The level of statistical significance was set at P < 0.05.

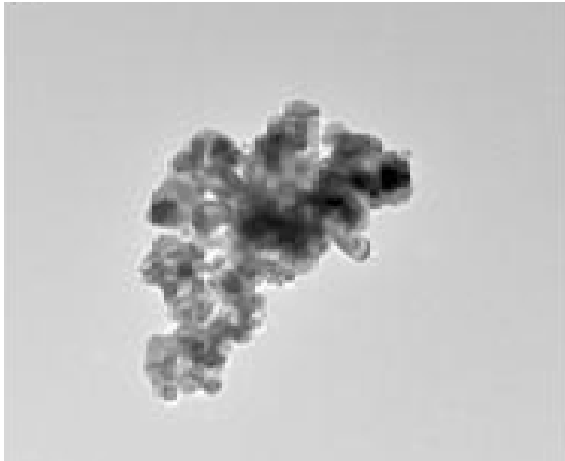
## 3. RESULTS



**3.1 UV-Vis Spectrophotometry** AgNPs exhibit optical properties due to their surface plasmon resonance (SPR) which depends upon shape, size and size distribution of the nanoparticles. The maximum wavelength was at 422.1 nm (Fig. 1).

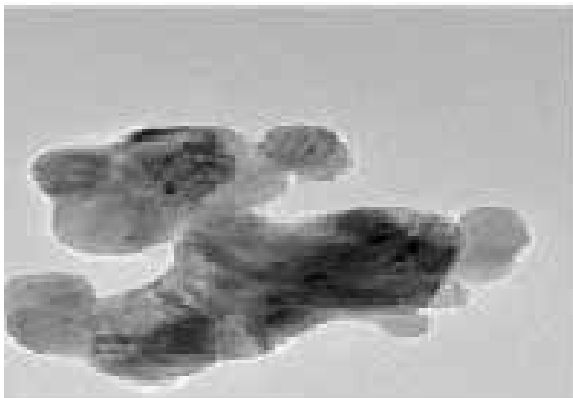
**Fig 1. UV-Vis spectrum of silver nanoparticles**  
**3.2 TEM (Transmission Electron Microscopy) Measurements**

The internal structure of the AgNPs was revealed in the TEM image and the average particle size was calculated to be around 50 nm (Fig. 2).



Dr Eman.008 50nm  
 print Mag×24000 Hv 80.0kv  
 Direct Mag ×24000

a)



Dr Eman.003 20nm  
 print Mag ×24000 HV80.01kv  
 Direct Mag ×24000

b)

**Fig. (2) Characterization of Ag NPs.** A-b represents the TEM characterization of Ag NPs .TEM ×24000

**3.3 Dynamic Light Scattering**

The effective diameter was found to be 46 nm by dynamic light scattering method in deionised water (Fig. 3).

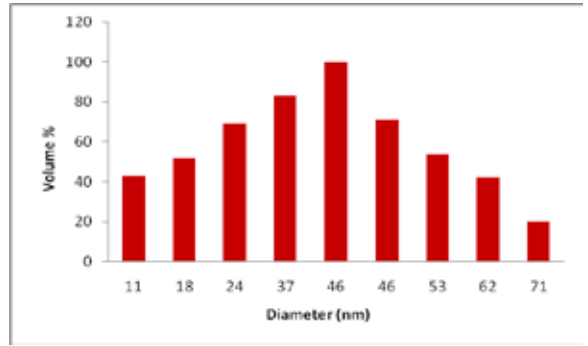


**Fig 3. Particle size distribution of silver nanoparticles in deionized water**

**3.4 FT-IR (Fourier transform Infra Red) Spectroscopystudies**

The FT-IR characteristic peaks for engineered AgNPs was at 660-682  $cm^{-1}$  (Fig. 4), the other characteristic peaks, were observed at 3434.98  $cm^{-1}$  represents amide-I region, 2923.56  $cm^{-1}$  for aldehyde groups and at 1627.69  $cm^{-1}$  which represents amide-II region.

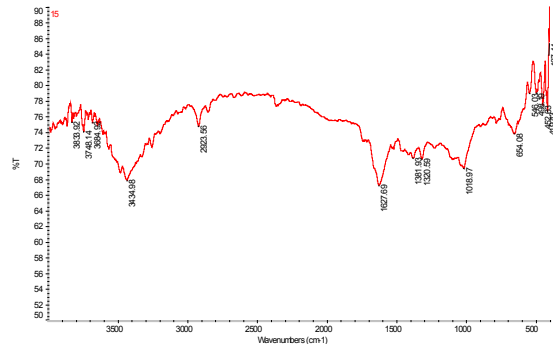


**Fig 4. FT-IR spectrum of Silver nanoparticles**

**3.5 Toxicity studies**

**3.5.1 Chromosomal aberrations**

The metaphase spreads shown in (Table 1) and Fig. 5Awas the control sample, in which no AgNP was added which resulted in a clean metaphase spread. At 5 $\mu g/mL$  of AgNP treated cell showed no appearance of aberrations on 24hr and 48hr exposure. The AgNP uptake was less and the metaphase chromosomes were normal. The aberrant cell percentage was zero. At 15 $\mu g/ml$  of AgNP treated cell showed tri-radial chromosomes with morphological alteration on 48 hr exposure (Table 1) and (Fig. 5B). The aberrant cell percentage was found to be 8%. The AgNP uptake has occurred the cell cycle has been arrested and chromosomal aberrations have been produced. At 25 $\mu g/ml$  of AgNP treated cell showed gaps and breaks on 24 hr and 48 hr exposure resulting in aberrant cell damage of 24% (Table 1) and (Fig. 5C). A minimum of 50 metaphases was scored per sample for the chromosome analysis.

**Table 1: Effect of AgNPs on human chromosomes on 24 & 48 hours exposure**

Ag NP ( $\mu g/mL$ )	Meta-phases analysed	Chromosome number	Fragments 24H/48H	Breaks 24H/48H	Gaps 24H/48H	Tri-radials 24H/48H	Aberrant Cell Damage (%)
		Mean $\pm$ SE					
5	50	46 $\pm$ 0	0	0	0	0	0
15	50	46 $\pm$ 0	0	0	0	0/ 4	8%
25	50	46 $\pm$ 0	0	5	7	0	24%

Ten healthy individual samples were analysed for 50 metaphases per concentration. Percentage of aberrant cells was expressed as number of cells which showed aberrations/ number of metaphases analysed × 100.

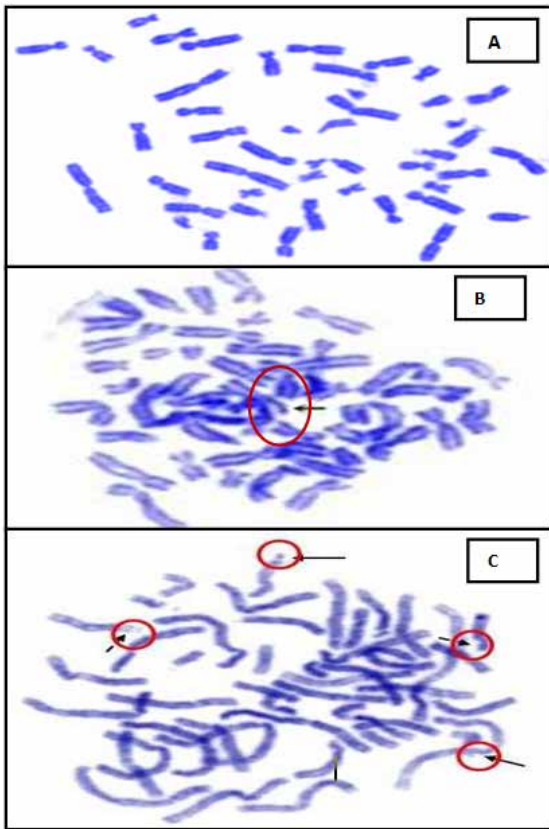


**Fig 5: Metaphase chromosomal aberrations at different concentrations of silver nanoparticles**  
 A – Healthy individual with no aberration (control), B- Metaphase spread with arrow mark indicates tri radial chromosome in 15 µg/mL of SNPs, C- Metaphase spread showing breaks, gaps and fragments (25µg/mL)

**3.6 Metal ion analysis**

The concentration of silver (Ag<sup>+</sup> ion) in cell culture medium and cell pellet was analysed (Table 2).

**Table 2: Ag<sup>+</sup> ion analysis of silver nanoparticles**

Concentration of silver nanoparticle added (µg/ml)	Total ion concentration (µg/ml) Mean± SD	
	In medium (RPMI-1640)	In cell pellet
25	1.166±0.02	3.169±0.16
15	0.725±0.02	1.859±0.03
5	0.211±0.01	0.605±0.01

**3.7 Haemolysis assay**

As shown in Fig. 6, haemolysis increased, sharply with the dose rising and the contact with plasma membrane occurs in haemolysis. The dose dependent haemolysis was better fitted by exponential curve fitting for AgNPs (Table3).

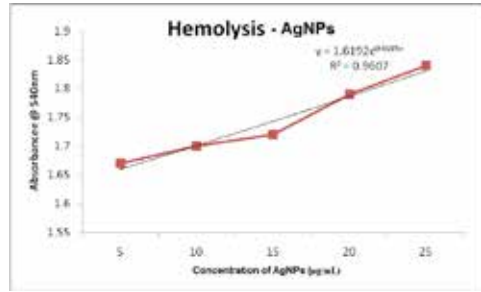


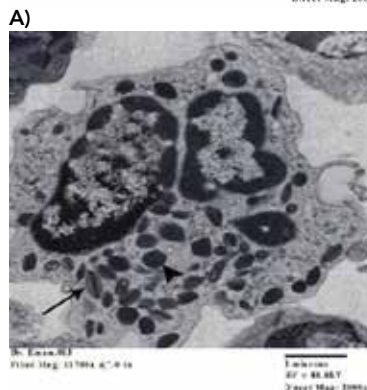
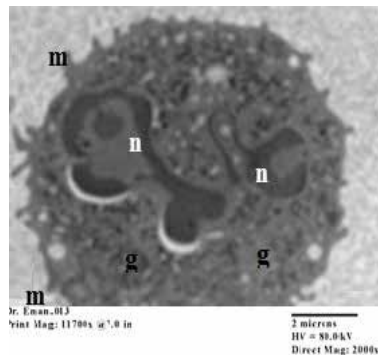
**Fig 6: Haemolysis of erythrocyte under AgNPs. The absorbance was measured at 540 nm**

**Table 3: the dose dependent haemolysis was better fitted by exponential curve fitting for AgNPs**

Trendline/ Regression	Function	R <sup>2</sup>
Linear	y = 0.043x+1.615	0.957
Exponential	y=1.619e <sup>0.024x</sup>	0.960
Logarithmic	y=0.099ln(x)+1.648	0.834
Power	y=1.65x <sup>0.057</sup>	0.842

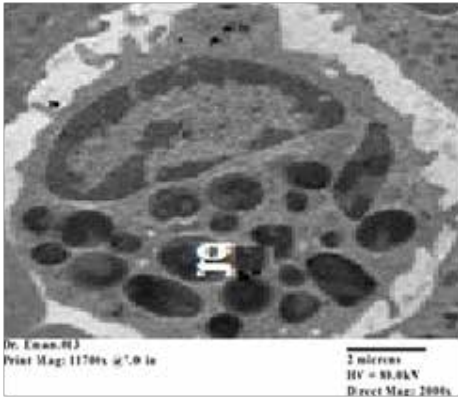
**3.4. Electron microscopic results:**

Ultrastructural analyses from control group (Fig. 7): illustrated a normal morphological appearance of the blood cells. Neutrophil with typical lobed nucleus and many granules were also observed within the cytoplasmic space, an eosinophil cella with segmented nucleus, condensed chromatin and large amount of granules of varying morphology and electron-density with a crystalloid structure in its cytoplasm were easily identified, a basophil revealed irregular round nucleus with sparse chromatin and eccentric nucleolus with heterogenous granules in the cytoplasm. a monocyte showed large indented nucleus and less electron dense cytoplasm and a lymphocyte revealed nuclear indentation .

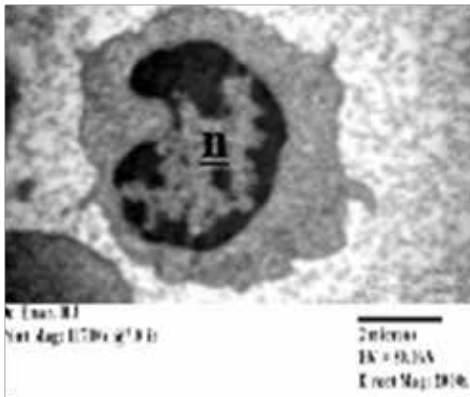


**B)**

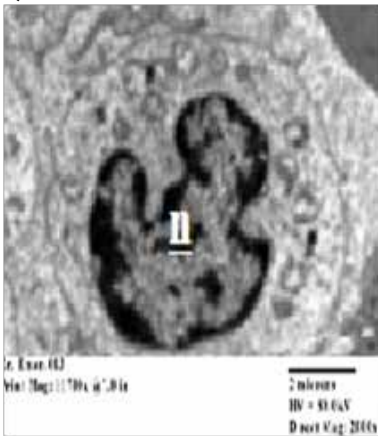




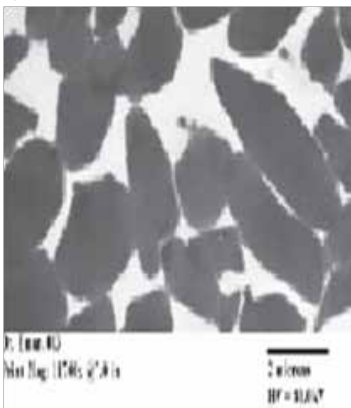
C)



D)



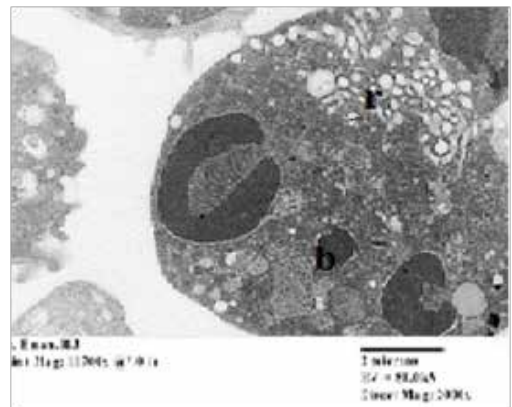
E)



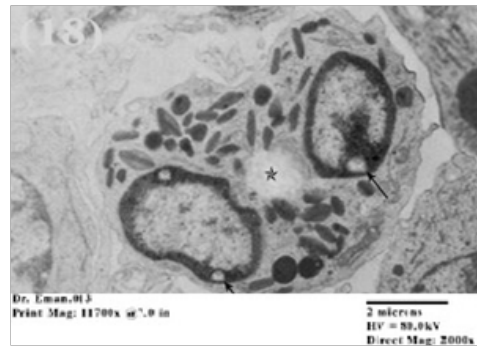
F)

Figure 7. A transmission electron micrograph from a control group showing A) a neutrophil showing numerous microvilli on its surface (m), lobulated nucleus (n) and cytoplasmic granules (g) TEM ×2000. B) An eosinophil with a cytoplasm filled with crystal-containing granules (arrow), dense azurophilic granules (arrowhead) and a segmented nucleus with heavily condensed chromatin (g) TEM ×2000. C) A basophil showing round nucleus with sparse chromatin and eccentric cytoplasmic granules (g) TEM ×2000. D) A monocyte showing deep indented nucleus (n) and less electron dense cytoplasm. E) A lymphocyte revealed nuclear indentation (n) TEM ×2000. F) normal concave shaped erythrocytes (n) TEM ×4000.

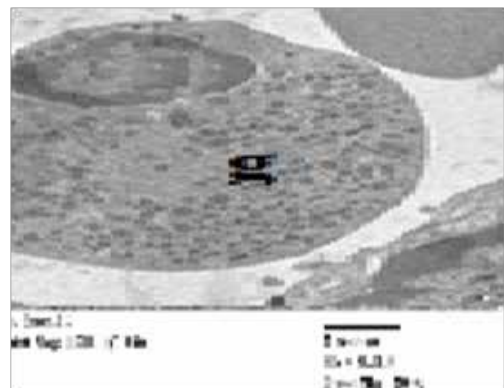
In contrast the other tested AgNPs toxicity group (Fig. 8) displayed marked alterations in the morphology of both red and white blood cells as neutrophils with cytoplasmic granules and nuclear chromatin condensation. Vacuolated less electron dense cytoplasm was noticed in other white cells. Compared with control (Fig.7), a change in the morphology of the red blood cells from concave to spherical was observed in (Fig. 8).



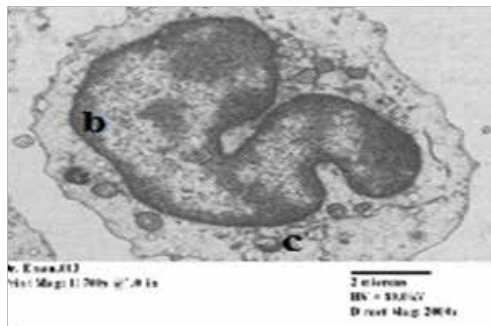
A)



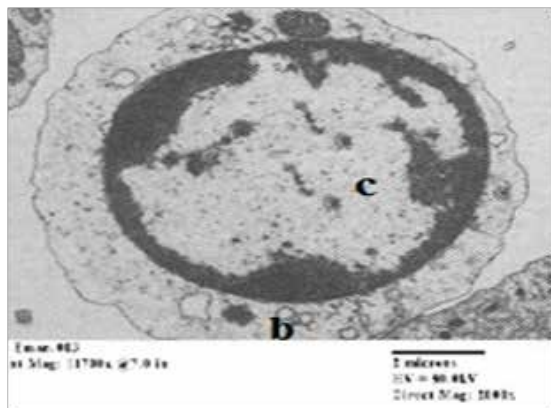
B)



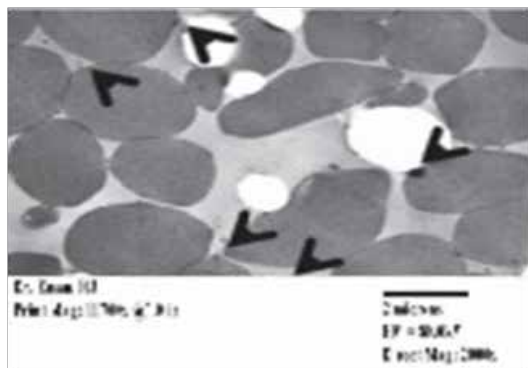
C)



D)



E)



F)

Figure 8. A transmission electron micrograph from AgNPs toxicity group showing A) an apoptosis of neutrophil in the form condensation of the cytoplasm with dilation of the endoplasmic reticulum (r). The nuclei show peripheral chromatin condensation and rounded bodies (b) TEM  $\times 2000$ . B) an eosinophil with intranuclear vacuole (arrows) with vacuolated (☆) less electron density cytoplasm, TEM  $\times 2000$ . C) A basophil showing nucleus with less electron dense granules in its cytoplasm (g) TEM  $\times 2000$ . D) A monocyte showing peripheral condensation of chromatin (b) and vacuolation of cytoplasm (c) TEM  $\times 2000$ . E) A lymphocyte revealed nuclear fragmentation (n) and vacuolation of cytoplasm (b) TEM  $\times 2000$ . F) destruction of erythrocyte integrity and hemolysis (arrow head) TEM  $\times 4000$ .

#### 4. DISCUSSION

Silver nanoparticles are widely used as bactericidal agents in consumer products, but their potential effects in humans remain poorly understood. Silver at doses below levels that cause argyria or argyriosis are generally considered to be relatively non-toxic<sup>(12)</sup>.

Johnston et al. 2010 have hypothesized that the toxic effects

of silver are proportional to free silver ions, but it is unclear how this relates to silver nanoparticles<sup>(26)</sup>.

The present study reveals that even at lower concentration of AgNPs, chances are available for induction of toxic effect on human cells. Also, an increase in DNA damage effect with higher AgNPs concentration.

Lee et al. 2013 separated the released Ag ions from the particles and measured their hepatotoxicity; they found a significant negative correlation between liver toxicity and AgNPs size<sup>(27)</sup>.

The uptake of nanoparticles inside human cell is still an unidentified area but there are probable mechanisms being suggested which sheds light to the mechanisms of toxicity as well as potential therapeutic application of nanoparticles. Attempts to identify the uptake routes of AgNPs led to the suggestion of: AgNPs were taken up primarily through endocytosis and diffusion<sup>(28)</sup>.

Johnston et al. 2010 suggested that AgNPs treated cells exhibit chromosome instability and mitotic arrest in human cells. Nanoparticle treated cells appeared to be clustered with a few cellular extensions which could be due to disturbances in cytoskeletal functions as a consequence of nanoparticle treatment<sup>(26)</sup>. When the AgNP uptake has occurred, the cell cycle has been arrested and chromosomal aberrations have been produced. In eukaryotic cells, DNA damage caused the arrests of cell cycle progression at the G<sup>2</sup>/M boundary, allowing cells extra time to repair damage prior to segregation of chromosomes<sup>(29)</sup>. Despite lesser uptake of silver ions by the blood cells, it proves to be toxic by producing chromosomal aberrations<sup>(21)</sup>. In vitro exposure of human peripheral blood cells to AgNPs in this study resulted in inhibition of PHA (Phyto-hemagglutinin) induced proliferation at a concentration  $\geq 15$   $\mu\text{g/ml}$ . Effects on cytokine production were already seen at non-cyto-toxic concentration of as low as 3  $\mu\text{g/ml}$ . In 25  $\mu\text{g/ml}$ , the AgNP treatment affects the cell cycle and mitotic index. This is a stable chromosomal aberration and AgNPs size influence the toxicity<sup>(27)</sup>.

This work brings out that: exposure of AgNPs resulted in chromosomal abnormalities, inhibition of proliferation that AgNPs have potential deleterious effect on erythrocyte in a dose-dependent way in vitro. The AgNPs were adsorbed to the erythrocyte membrane due to their high surface-volume ratio. Once the surface was covered by AgNP, erythrocyte showed a tendency to be agglutinated because the membrane-bound AgNP deformed erythrocyte and hence decreased the repulsion among erythrocytes.

The erythrocyte membrane is composed of a lipid bi-layer primarily with protein embedded in, which keeps the membrane in dynamic equilibrium between fluidity and solidity. Erythrocyte is extremely vulnerable to oxidative damage because of the high poly-unsaturated fatty acid content in the membranes. The high active molecule ultimately leads to the decrease of erythrocyte survival through induction of haemolysis<sup>(30)</sup>.

Tiwari et al. 2011<sup>(31)</sup> assessed increased single and double DNA breakage in rats after intravenous injection of 40 mg kg<sup>-1</sup> bw of Ag NPs. In the second in vivo study, zebrafish were treated with oral Ag NPs (5 nm to 20 nm), which resulted in high levels of  $\gamma$ -H2AX - a marker for double DNA strand breaks. Moreover, the exposure to AgNPs resulted in a non-significant dose-dependent increase in hepatic p53 mRNA the precursor of the tumour suppressor protein and an indirect DNA damage marker<sup>(32)</sup>.

In the present study also, the toxic effects of AgNPs on human peripheral blood lymphocytes had been examined. It is shown that the AgNPs could produce fragments and gaps as a result of ROS generation and increased ROS levels leading

to DNA damage. It is yet to be elucidated whether the toxic effects of AgNPs are specific to any chromosome, or any type of nanomaterials would have similar effects on chromosomes.

Erythrocytes are incapable to produce SOD and catalase, hence are vulnerable to the extraneous toxicants since the cell membrane may be easily damaged during lipid peroxidation. Haemolysis resulted from the breakage of erythrocyte membrane exposed to AgNPs which happened when the content escaped from the inner to the outer of erythrocyte. Metallothioneins are regarded as essential biomarkers in metal-induced toxicity which facilitates metal detoxification and protection from free radicals<sup>[24, 26]</sup>.

Examinations of TEM images reveal that AgNPs were lead to ultra-structural morphological changes in all types of blood cells in the form of cytoplasmic granules and nuclear chromatin condensation in white blood cells indicated cell death with change in the morphology and destruction of red blood cells membrane, this explains by Nanoparticle interactions with erythrocytes cause abnormal membrane proteins and lipids that lead to the destruction of erythrocyte integrity and hemolysis. Qiang et al. 2008 found that nanoparticle interactions with erythrocytes cause abnormal membrane proteins and lipids that lead to the destruction of erythrocyte integrity and hemolysis<sup>[29]</sup>.

Nanoparticles can usually be internalized within cancer cells as well as by many other primary cells. However, in this study, all the silvernanoformulations failed to internalize in erythrocytes but instead attached to the membranes of the red blood cells. This mainly occurs as a result of interaction between the silver and the protein components of the plasma membrane, causing a change in the properties of the red cell membrane<sup>[33,34]</sup>.

Further, karyotyping studies are to be carried out for locating the aberration thereby using it as a "potential marker" fragment which can be restricted and used in onco-therapy. In depth studies are needed to assess the risks of AgNPs and to comprehend the underlying mechanisms.

## CONCLUSION

This research validates that even at 15 µg/mL concentration of AgNPs has the potential to cause toxicity as analyzed by a range of cyto and genotoxicity parameters. The chromosomal aberrations and cell cycle arrest issues the safety related to AgNPs. Chromosomal aberrations are believed to be the key factors resulting in cell cycle arrest. Prospective application of AgNPs as an anti-proliferative agent could be narrowed by the fact that it is similarly toxic to normal cells. The mitotic arrest of cells at G<sup>2</sup>/M boundary can be further investigated on onco-therapy. Besides embracing the antimicrobial potential, the biological applications employing AgNPs should be given special attention for its toxicity.

## COMPETING INTERESTS:

### I. FINANCIAL COMPETING INTERESTS

1. In the past five years I have NOT received reimbursements, fees, funding, or salary from an organization that may in any way gain or lose financially from the publication of this manuscript, either now or in the future.
2. I DON'T hold any stocks or shares in an organization that may in any way gain or lose financially from the publication of this manuscript, either now or in the future.
3. I DON'T hold or applying for any patents relating to the content of the manuscript.
4. I DON'T received reimbursements, fees, funding, or salary from an organization that holds or has applied for patents relating to the content of the manuscript.
5. I DON'T have any other financial competing interests.

### II. NON-FINANCIAL COMPETING INTERESTS

There is a non-financial competing interest (personal, and academic) to declare in relation to this manuscript which is promotion in work.

## AUTHORS' CONTRIBUTIONS

Author (1, 2) participated in the design of the study, writing the manuscript and performed the statistical analysis. Author (3) carried out the molecular genetic studies, EM examination of the specimens, participated in the sequence alignment and drafted the manuscript. Author (4, 5) carried out the cell culture part.

Author (3-5) participated in the sequence alignment. Author (1, 2) conceived of the study, and participated in its design and coordination and helped to draft the manuscript. All authors read and approved the final manuscript.

ACKNOWLEDGEMENTS 'We thank RaniaHamdyAfify who help in statistical analysis of this work. The authors had depend on their own in financial support of their work. We acknowledge the language editor "....." who had made significant revision of the manuscript.'

## REFERENCE

1. Landsiedel, R; Kapp, MD.; Schulz, M; Wiench, K; Oesch, F. Genotoxicity investigations on nanomaterials: Methods, preparation and characterization of test material, potential artefacts and limitations—Many questions, some answers. *Mutat. Res. Rev. Mutat. Res.*, 2009; 681, 241-258. | 2. Singh, N; Manshian, B; Jenkins, GJS; Griffiths, MS.; Williams, MP; Maffei, GGT; Wright, JC.; Doak, HS. NanoGenotoxicology: The DNA damaging potential of engineered nanomaterials. *Biomaterials*, 2009; 30, 3891-3914. | 3. Osterberg, R; Persson, D; Bjursell, G. The condensation of DNA by chromium (III) ions. *Biomol Struct Dyn.*, 1984; 2, 285-290. | 4. The Royal Society and Royal Academy of Engineering, UK. Nanoscience and Nanotechnology, Opportunities and Uncertainties. UK: The Royal Society; 2004 | 5. Munzuroglu, O; Geckil, H. Effects of metals on seed germination, root elongation, and coleoptile and hypocotyl growth in *Triticum aestivum* and *Cucumis sativus*. *Arch. Environ. Contam. Toxicol.*, 2002; 43, 203-213. | 6. Oberdorster, G; Oberdorster, E.; Oberdorster, J. Nanotoxicology: an emerging discipline evolving from studies of ultrafine particles, *Environ. Health. Perspect.*, 2005; 113, 823-839. | 7. Anastasio, C ; Martin, ST.; Atmospheric nanoparticles. *Rev Miner Geochem.*, 2001; 44, 293-349. | 8. Nel, A; Xia, T; Madler, L; Li, N. Toxic potential of materials at the Nanolevel, *Science*, 2006; 311, 622-627. | 9. Kahru, A; Dubourgier, HC. From ecotoxicology to nanoecotoxicology, *Toxicology*, 2010; 269, 105-119. | 10. Chen, X; Schluessener, H.J. Nanosilver: a nanoparticle in medical application. *Toxicol Lett.*, 2008; 176, 1-12. | 11. Tripathy, A; Chandrasekran, N; Raichur, AM; Mukherjee, A. Antibacterial applications of silver nanoparticles synthesized by aqueous extract of *Azadirachta indica* (Neem) leaves. *J Biomed Nanotech.*, 2008; 4, 1-6. | 12. Toxicological profile for Silver. Contract No: 205-88-0608. Prepared by Clement international corporation, U.S. Public Health Service, ATSDR/TP-90-24. ATSDR (Agency for toxic substances and Disease Registry) 1990. | 13. Park, EJ; Yi, J; Kim, Y; Choi, K; Park, K. Silver nanoparticles induce cytotoxicity by a Trojan-horse type mechanism, *Toxicol in Vitro.*, 2010; 24, 872-878. | 14. Miura, N; Shinohara, Y. Cytotoxic effect and apoptosis induction by silver nanoparticles in HeLa cells. *Biochem. Biophys. Res. Commun.*, 2009; 390, 733-737. | 15. Helland, A. In: Nanoparticles: A closer look at the risks to human health and the environment, IIIIEE(The International Institute for Industrial Environmental Economic), Lund University, Sweden. 2004:1-98. | 16. Monteiroa, DR.; Gorupb, LF; Takamiyaa, AS.; Ruvollo, AC.; Camargob, ER.; Barbosaa, DB. The growing importance of materials that prevent microbial adhesion: antimicrobial effect of medical devices containing silver. *Int J Antimicrob. Ag.*, 2009; 34, 103-110. | 17. Rai, M; Yadav, A; Gade, A. Silver nanoparticles as a new generation of antimicrobials, *Biotech Adv.*, 2009; 34, 76-83. | 18. Eom, HJ.; and Choi, J. Activation, DNA Damage, Cell Cycle Arrest and Apoptosis As Mechanisms of Toxicity of Silver Nanoparticles in Jurkat T Cells. *Environ. Sci. Technol.*, 2010; 44, 8337-8342. | 19. Sathya, TN.; Vardhini, NV.; Balakrishnamurthy, P. Revolution of Nano in in-vitro genetic toxicology, *Cell and Tissue Res.*, 2010; 3, 2389-2396. | 20. Ramos, DL.; Gaspar, JF.; Pingarilho, M; Gil, OM.; Fernandes, AS.; Rueff, J; Oliveira, NG. Genotoxic effects of doxorubicin in cultured human lymphocytes with different glutathione S-transferase genotypes, *Mutat Res. Genetic Toxicol. Environ Mutagenes.*, 2011; 724, 28-34. | 21. AshaRani, PV.; Hande, MP.; Valiyaveetil, S. Anti-proliferative activity of silver nanoparticles. *BMC Cell Biology.*, 2009; 10, 65. | 22. Lin, D; Xing, B. Root uptake and Phytotoxicity of ZnO nanoparticles, *Environ Sci Technol.*, 2008; 42, 5580-5585. | 23. Wang, HH.; Wick, RL.; Xing, BS.; Toxicity of nanoparticles and bulk ZnO, Al<sub>2</sub>O<sub>3</sub> and TiO<sub>2</sub> to the nematode *Caenorhabditis elegans*. *Environ Pollut.*, 2009; 157, 1171-1177. | 24. Hebbel, RP.; Leung, A; Mohandas, N. Oxidation-induced changes in micro-rheologic properties of the red blood cell membrane. *Blood.*, 1990; 76, 1015-1020. | 25. Bozzola J. J., and Russell L. D. Specimen preparation, staining and photomicrograph production for transmission electron microscope(TEM). In: *Electron Microscopy, ions and Barlett's publisher International, UK, 2nd Edition. 1999* | 26. Johnston HJ, Hutchison G, Christensen FM, Peters S, Hankin S, Stone V. A review of the in vivo and in vitro toxicity of silver and gold particulates: particle attributes and biological mechanisms responsible for the observed toxicity. *Crit Rev Toxicol* 2010;40:328-46. | 27. Lee Y. , Liu M., Huang L., Lue S., Lin L., Kwan A. and Yang R. Bioenergetic failure correlates with autophagy and apoptosis in rat liver following silver nanoparticle intraperitoneal administration, *Particle and Fibre Toxicol.* 2013, 10(40):1-13. | 28. Shin, SH.; Ye, MK.; Kim, HS.; Kang, HS. The effects of nano-silver on the proliferation and cytokine expression by peripheral blood mononuclear cells. *Int Immunopharmacol.*, 2007; 13, 1813-1818. | 29. AshaRani, PV.; Grace Low, KM.; Hande, MP.; Valiyaveetil, S. Cytotoxicity and Genotoxicity of Silver Nanoparticles in Human Cells, *ACS Nano*, 2009; 3, 279-290 | 30. Qiang, LS.; Rong, Z; Hong, Z; Meng, X; Yu, SX.; De, YS.; Long, W.S. Nanotoxicity of TiO<sub>2</sub> nanoparticles to erythrocyte in vitro, *Food Chem Toxicol.*, 2008; 46, 3626 -3631. | 31. Choi JE, Kim S, Ahn JH, Youn P, Kang JS, Park K, Yi J, Ryu DY. Induction of oxidative stress and apoptosis by silver nanoparticles in the liver of adult zebrafish. *Aquat Toxicol* 2010;100:151-9. | 32. Tiwari DK, Jin T, Behari J. Dose-dependent in vivo toxicity assessment of silver nanoparticle in Wistar rats. *Toxicol Mech Methods* 2011;21:13-24. | 33. Klien K, and Godni -Cvar J. Genotoxicity of Metal Nanoparticles (Focus On In Vivo Studies), *Arh Hig Rada Toksikol* 2012;63:133-145. | 34. Duchnowicz, P; Koter, M; Duda, W. Damage of erythrocyte by phenoxyacetic herbicides and their metabolites. *Pestic. Biochem. Physiol.*, 2002; 74, 1-7. |